An Active Position Sensing Tag for Sports Visualization in American Football

Darmindra D. Arumugam[1], Michael Sibley[2], Joshua D. Griffin[3], Daniel D. Stancil[4], David S. Ricketts[5]
[1]Jet Propulsion Lab., California Institute of Technology, Pasadena, CA, Email: Darmindra.D.Arumugam@jpl.nasa.gov
[2]Tait Towers, Lititz, PA, Email: mike.sibley@gmail.com
[3]Disney Research, Pittsburgh, PA, Email: joshdgriffin@disneyresearch.com
[4,5]North Carolina State University, Raleigh, NC, Email: [4]ddstancil@ncsu.edu [5]david.ricketts@ncsu.edu

***Abstract*—Remote experience and visualization in sporting events can be significantly improved by providing accurate tracking information of the players and objects in the event. Sporting events such as American football or rugby have proved difficult for camera- and radio-based tracking due to blockage of the line-of-sight, or proximity of the ball to groups of players. Magnetoquasistatic fields have been shown to enable accurate position and orientation sensing in these environments [1]–[3]. In this work, we introduce a magnetoquasistatic tag developed for tracking an American football during game-play. We describe its integration into an American football and demonstrate its use in game-play during a collegiate American football practice.**

I. Introduction

The use of camera-based and wireless localization technology in sports is growing for application such as athlete training, game analysis, and visualization [4]. However, localization in many sport environments is challenging because the line-of-sight (LoS) to the person/object to be tracked can be blocked by the bodies of players. This situation is common for ball tracking in American football or rugby where the ball can be buried under several player's bodies or held close to a player's body. In such situations, localizing the ball with a camera is difficult and conventional localization systems, such as ultra-wideband (UWB), satellite-based, and backscatter radio frequency identification (RFID), will suffer reduced accuracy.

In an effort to meet these challenges, a tracking system based on magnetoquasistatic fields has been developed, and studied in detail, to determine both the position and orientation of a sensor when the LoS is blocked and the sensor is close to lossy dielectrics (e.g., player's bodies) [1]–[3], [5]. The tracking system measures the magnitude of the magnetic field generated by a small magnetic dipole antenna at multiple spatial location and then inverts the field equations to determine the sensor's position and orientation.

In this paper, we characterize the active RF tag for use in magnetoquasistatic position sensing of an American football during actual game-play. The tag is integrated into an American football and its operation presented during an actual play. The technique, algorithm, and accuracy have been previously reported for the one-dimensional (1D) case in [1], two-dimensional case in [5], three-dimensional case in [2], and for a goal-line play in [3]. In [1], we demonstrated a 1D distance estimation error 11.74 cm for distances between 1.3 and 34.2 m, whereas in [2], we showed a mean 3D position error of 0.77 m, a mean inclination orientation error of 9.67°, and a mean azimuthal orientation error of 2.84°.

D.D. Arumugam and M. Sibley performed this work at Disney Research.

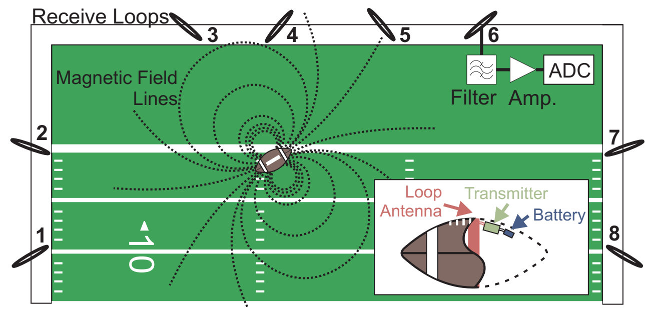

Fig. 1. Magnetoquasistatic positioning system setup. The football is equipped with an integrated transmitter that emits quasistatic magnetic fields. Eight receivers, positioned around region of the field extending from the back of the end-zone to the ten yard line, were used to track the ball from the back of the end-zone to approximately the 15 yard line.

A brief overview of the system is provided in Section II and the design of the active RF tag is discussed in Section III. The ball's integration into a football is presented in Section IV; the integrated tag's performance under various conditions is discussed in Section V; and a preliminary study of the specific absorption rate (SAR) induced in an adult male is reported in Section VI. Finally, results from the system's use in a collegiate football practice are presented in Section VII.

II. System Design

The magnetoquasistatic tracking system is shown in Fig. 1. An electrically-small loop, or transmitter, is used to preferentially excite magnetoquasistatic fields that are sensed by multiple receiving antennas whose positions and orientations are known. By knowing the magnetic moment of the transmitter, the position and orientation of the transmit loop can be determined using the governing field equations and a least-squares solver [1], [2].

In the American football application, there are several requirements for the tracking system. The first is that the receive antennas must be placed out of the active playing field, resulting in a maximum transmitter-to-receiver distance of approximately 50 m. The second is that the transmitter must be seamlessly integrated into the football so as not to disturb its performance, in particular the transmitter's weight

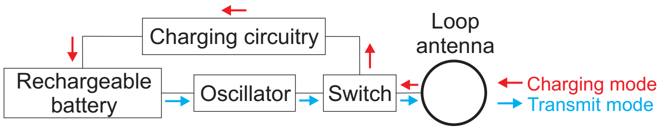

Fig. 2. Block diagram of the magnetoquasistatic tag and loop antenna.

should be less than the variation of an average football, which is approximately 28 g [6]. Finally, the transmitter must be durable and accurate to provide tracking during play, when the football may be under physical stress, e.g., the weight of a body as well as when in close proximity to the player's bodies.

Our approach is shown in Fig. 1, where the loop is coiled around the air-bladder of the football, and the circuit and battery are located between the air-bladder and the outer leather enclosure. Here, we define the football coil antenna, associated circuitry and battery as the RF tag as shown in Fig. 2. The choice of tag operating frequency is determined by two competing requirements: 1) the quasistatic region ($\ll \lambda$, where λ is the wavelength of the magnetic field) must be large and is achieved using a low frequency (which also reduces the effects of small, interfering objects and players); and 2) a strong coupling between the transmitter and receivers is required for a good signal-to-noise ratio (SNR), which can be achieved at a higher frequency. We choose a frequency of approximately 400 kHz to balance these two requirements and stay below the AM broadcast band [1].

III. Football Tag Design

The transmitter integrated into the American football consists of an oscillator circuit connected to a multi-turn loop antenna. The oscillator circuit is powered by a rechargeable battery that is inductively charged using the same antenna as shown in Fig. 2. Since the integrated transmitter must not disturb the dynamics of the ball during game-play, care must be given to the placement and weight of the integrated transmitter. The weight of the battery, circuitry, and antenna were chosen to be less than the weight tolerance of an American football (28 g) used in the National Football League [6].

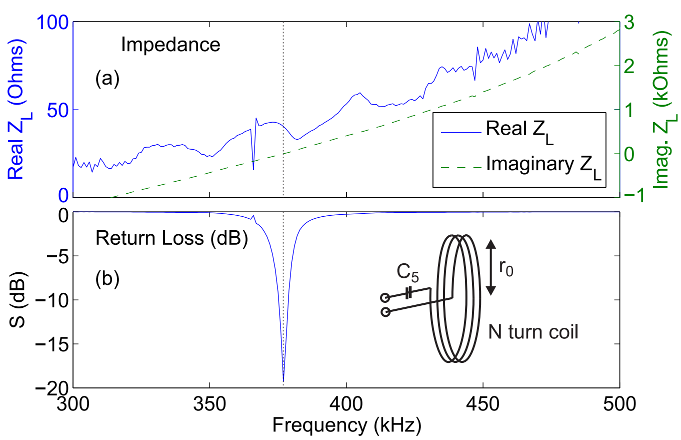

Fig. 3. Impedance of the coil used as the transmitting loop antenna is shown in (a). The inset of (a) shows the multi-turn coil and capacitor for the antenna, where r_0=8.25 cm, and N = 45. The capacitor, which is labeled C_5 in Fig. 5, was chosen to resonate the inductance of the loop at 376 kHz. The return loss is shown in (b).

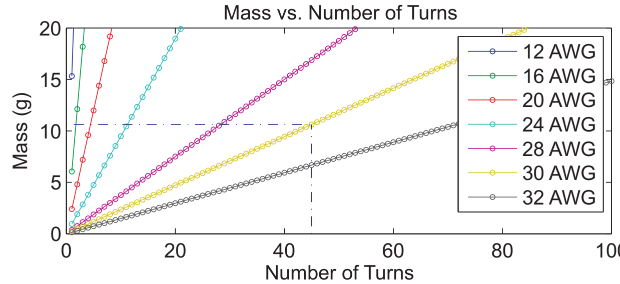

Fig. 4. Mass of the coil antenna as a function of the number of loop turns.

A. Antenna Design

To preferentially excite a magnetic field, a coiled loop antenna was used with the transmitter. The antenna was coiled around the air-bladder and underneath the outer leather of the football as shown in the inset of Fig. 1. It consisted of a multi-turn loop as depicted in the inset of Fig. 3. The coil antenna had a radius, r_0, of 8.25 cm to accommodate the radius of the American football. We used 45 turns of closely wound, 30 AWG (American Wire Gauge) wire to limit the weight to 10.33 g, and resonated the loop inductance with a series capacitor to obtain a resonant frequency of approximately 376 kHz. The real and imaginary impedance of the resonant loop antenna, measured using a vector network analyzer (VNA), is shown in Fig. 3a. The measured return loss, shown in 3b, verifies the resonant frequency of 376 kHz.

Figure 4 shows the calculated mass of the coil antenna as a function of number of turns. The dashed lines indicate values for the 45-turn coil using 30 AWG wire, as used in the design. The magnetic moment of the coil antenna is dependent on the number of turns and current flowing through those turns. As we increase the number of turns, we must increase the wire gauge to maintain our target weight of approximately 10g. A higher wire gauge leads to a larger resistance, which reduced current when a class-E source is used. Thus, there is a diminishing return on increasing the number of turns and we found 45 turns to be a good design point. A complete optimization of turns and gauge is the subject of future work.

B. Oscillator Circuit

The principle requirements of the football oscillator are that it be lightweight, have high efficiency, and have relatively high output power. Through experimentation, we found that an output power of approximately 0.5 W was required to achieve adequate SNR for distances up to the width of the American football field. We satisfied these requirements using a 45-turn coil loop antenna driven by a class-E oscillator circuit with power supplied through a 3.3V rechargeable battery, as shown in Fig. 5. A high-efficiency class-E design procedure

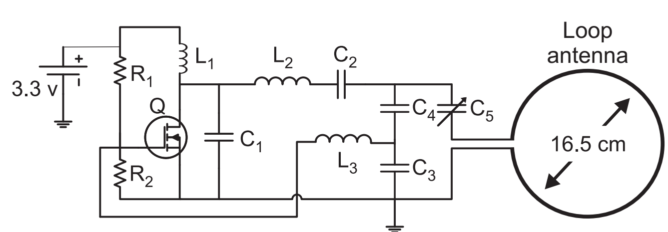

Fig. 5. The class-E oscillator circuit design used for the transmitter.

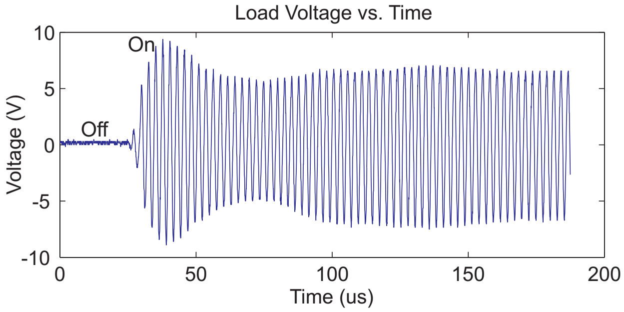

Fig. 6. Transient load voltage measured at the terminals of the 45-turn coil antenna connected to the output of the class-E oscillator.

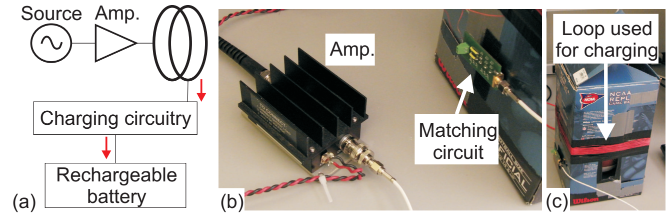

Fig. 8. The charging system block diagram is shown in (a). A photo of the setup is shown in (b), where the output impedance of the amplifier was matched to the loop using matching circuit. A photo of the secondary loop wrapped around a box and used for charging is shown in (c). The integrated football was placed inside the box during charging.

[7] was used to obtain an oscillation frequency and efficiency of 376 kHz and 93%, respectively, with an output power of 0.56 W and a current of 159 mArms flowing through the coil antenna [5].

To study the transient characteristics, the antenna was connected to the output terminal of the oscillator and the transient characteristic of the load voltage across the antenna terminals was measured using a high-impedance digital oscilloscope, shown in Fig. 6. The oscillator load voltage required approximately 15-20 μs and 90-100 μs to achieve the 25% and 10% margin of error in voltage (stable to within 75% and 90%, respectively), respectively.

To accommodate reuse, the oscillator circuit is powered with a rechargeable battery and charging is accomplished by adding circuitry that receives energy through the transmit loop antenna, shown in Fig. 7a. A surface mount switch is used to change the circuit from transmitting mode to charging mode and charging occurs when the integrated ball is placed in close proximity to a secondary transmitting loop as shown in Fig. 8. The charging circuitry consists of a full-wave bridge rectifier, a voltage regulator, and a microcontroller to enable lithium-polymer battery charging. The fabricated and populated complete circuit with charging and oscillator is shown in Fig. 7b. The rechargeable battery used for the football application was a lithium-polymer type (PRT-10718 by Sparkfun), with a capacity of 400 mAh, a maximum current draw of 800 mA, and a weight of 9 g. The populated circuit board weighed a total of 7.18 g and had a dimension of 39.5 mm $\times$ 33.0 mm. The total RF tag weight was 26.51 g, which is below the 28 g requirement. This included the antenna, oscillation and charging circuitry, and rechargeable battery.

To study the drain characteristics, the battery was fully charged and drained by switching the circuit to the transmit mode. Figure 9a shows a plot of the voltage as a function of time in the transmit mode, measured at the terminals of the battery. The battery capacity and maximum current draw allows for uninterrupted use of the football transmitter for a period of approximately 4 hours and 45 minutes. By switching to charging mode, the circuit stops behaving as a transmitter and instead converts any induced currents into energy to recharge the battery. A secondary loop connected to a signal generator through an amplifier was used to supply the inductive field during charging, as shown in Fig. 8. The signal generator's output power of +10 dBm was used along with +30dB of amplification to achieve +40dBm output to the terminals of the resonant loop (made of 100 turns of 30 AWG wire) at approximately 538 kHz. The charging coil was wrapped around a football packaging box with a dimension of approximately 17 cm x 17 cm. The integrated ball was placed inside the box to charge it's battery. Both the charging and transmitting loops were placed parallel to each other and at a separation of approximately 2 cm. Figure 9b shows a plot of the voltage as a function time in charging mode, measured at the terminals of the battery. The inductive charging takes approximately 13 hours and 40 minutes to fully charge the rechargeable battery in the present configuration. This rather lengthy time is due to the high-loss of the charging loop and a non-optimized impedance match between the charging source and load. It was suitable, however, for overnight charging, as needed for testing.

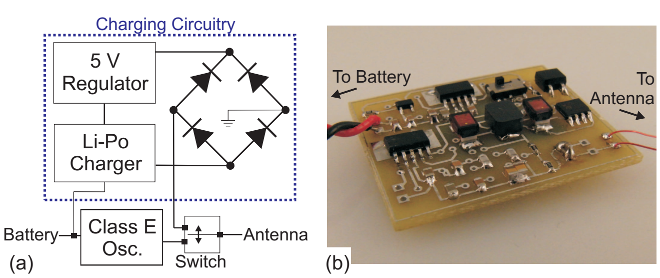

Fig. 7. The transmitting circuit equipped with a charging circuitry to allow for wireless charging of the rechargeable battery is shown in (a). The fabricated and populated circuit with integrated wireless charging is shown in (b).

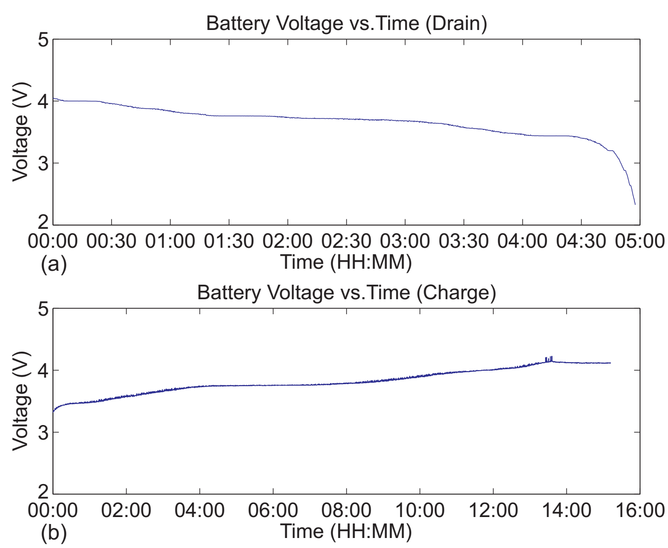

Fig. 9. Drain (a) and charge (b) characteristics as a function of time for the integrated oscillator with charging circuitry.

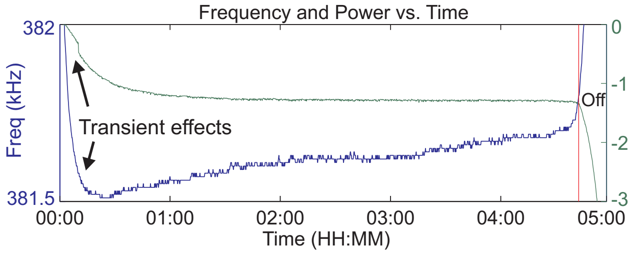

Fig. 10. Measured power and frequency as a function of time for the integrated transmitting circuitry. Initial transient effects are observed within the first 15 min., which are likely caused by internal heating.

C. Tag Operation

Figure 10 shows measurements of the relative power and frequency of the emitted magnetic field as function of time. The magnetic field is measured using a co-polarized receive antenna (model LFL-1010 from Wellbrook Communications) at a distance of approximately 2 m from the football transmitter and a spectrum analyzer with a resolution bandwidth of 300 Hz. Initial transient effects show rapidly changing received power and center frequency within 15-20 minutes of the turn-on time. Therefore, tags were used after an approximately 25-minute warm-up period. The tag shows a total stable operation time of approximately 4 hours, which safely covers operation over the length of an entire football game. The oscillation frequency is found to be approximately 381.6 kHz, which is different from the antenna resonance and circuit design, which was 376 kHz. This is due variability in components from one board to another, and due to changes in oscillation characteristics after integration into an American football.

IV. Integration into an American Football

The integration of the magnetoquasistatic tag into the football required placement of the transmit loop, circuitry, and battery inside the football so that it could be used unhindered during game-play. A commercially-available reproduction of an NFL football was used for the integration. The football was constructed of a leather outer shell, a rubber air bladder, and a plastic lacing to seal the ball. To integrate the magnetoquasistatic tag, the football was first deflated and carefully deconstructed. The lacing was untied (Fig. 11a) and the additional stitching holding the ball opening was cut (Fig. 11b). The rubber bladder and the air nozzle were also removed from the leather shell (Fig. 11c). The air bladder, now free from the leather shell, was re-inflated to match the inside dimension of the shell. The purpose of re-inflation was to allow the emitting loop to be wrapped around the air bladder. The loop was wrapped around the small diameter of the air bladder and the plane of the loop was orthogonal to the long axis of the ball (Fig. 11d). Cloth-backed adhesive tape was used to prevent the antenna from shifting on the flexible rubber surface. Another layer of tape was placed on top of the antenna and the assembly was taped to the rubber bladder at several intervals to prevent the antenna from shifting while being installed. The bladder and antenna were then inserted under the leather shell as outlined in the following steps: First, the bladder was deflated and the air nozzle was reinserted through the existing hole (Fig. 11e). Next, the remainder of the bladder was fed through the opening into the ball and partially inflated. The oscillator circuit was attached to the loop and the system tested. Next, the transmitter circuitry was covered with epoxy to protect it during use, and was then placed along with the battery inside the ball (Fig. 11f). The circuit was secured with glue to the inside of the leather to prevent shifting while in use. To allow access to the switch, it was positioned below one of the existing holes for the football lacing, where it could be accessed using tweezers or a similar tool. The football lacing was then replaced (Fig. 11g) and the ball was fully inflated.

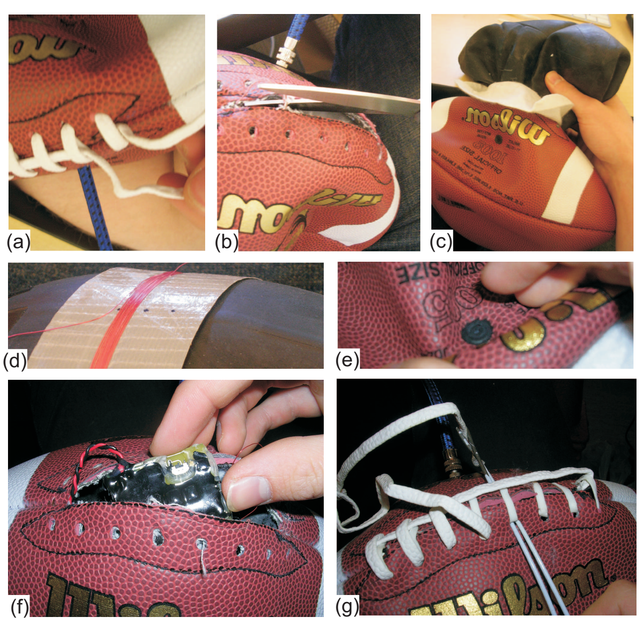

Fig. 11. Integration of the transmitting circuitry, loop antenna, and rechargeable battery into the American football.

V. Performance in Football

The integrated football was put through a series of tests in order to ensure its stability and study its performance during game-play. These tests measured signal variations with different air pressures, force loading on the football, dielectric

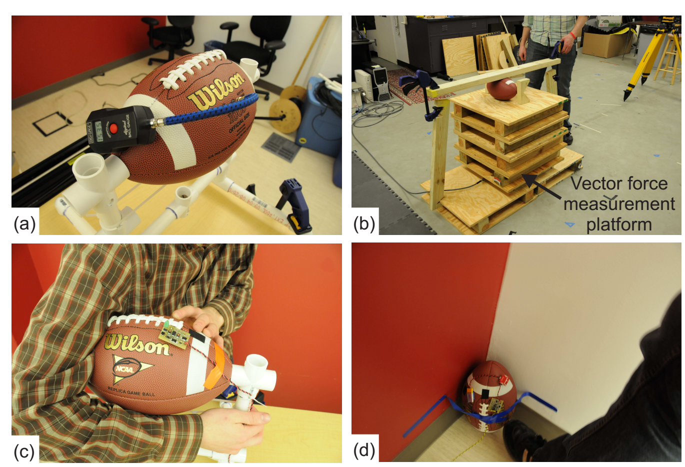

Fig. 12. Experiments conducted to determine the performance of the integrated football: The football air-pressure test is shown in (a); The force test is shown in (b); The dielectric (human hand/arm) loading test is shown in (c); The kick (or impact) test is shown in (d).

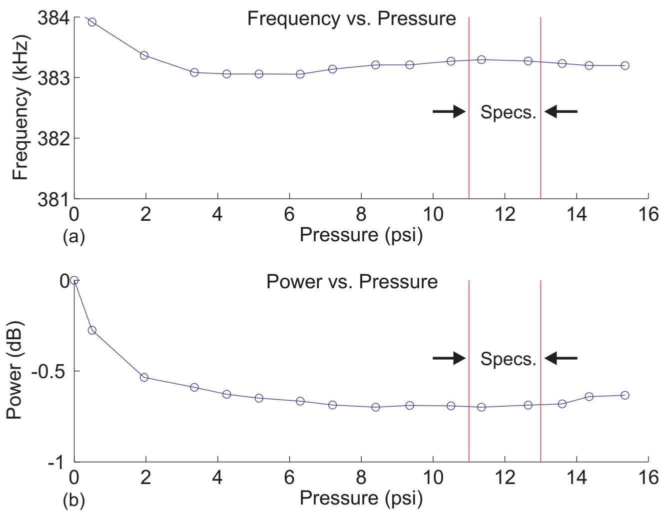

Fig. 13. The result of the football air-pressure test, showing the measured frequency (a) and power (b) as a function of internal football air pressure. The red vertical lines indicate the specifications for air pressure in the NFL [6].

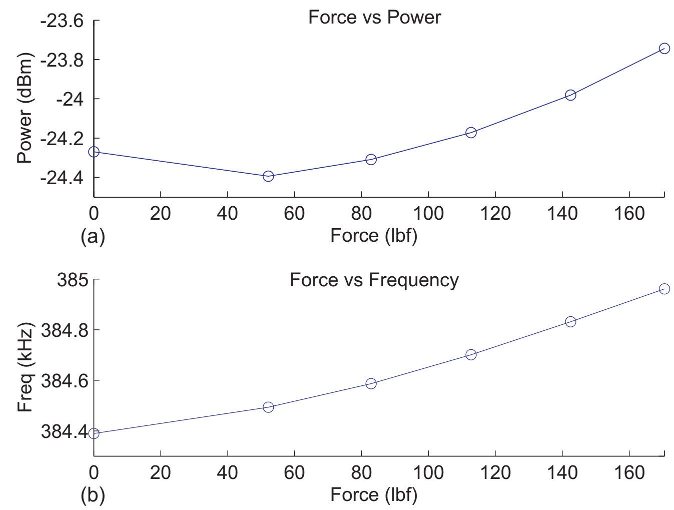

Fig. 14. The result of the force test, showing the measured power (a) and frequency (b) as a function of applied force onto the ball.

loading (i.e., the proximity of the hand and arm) on the football, and impact (i.e., the effect of a kick or drop) applied to the football. The configuration and setup for each test is shown in Fig. 12 and is described in the following sub-sections.

A. Pressure Test

Since the transmitting loop antenna was wound around the air bladder, the inflation pressure of the ball could affect the transmitter's performance. To examine this effect, the ball was placed on a fixed mount, as seen in Fig. 12a, and the frequency and power of the ball were measured at various inflation pressures. A wide range of pressures were tested, shown in Fig. 13, well below and above the permissible air pressure allowed by NFL regulations [6]. A digital air pressure gauge (model AG500 by Mikasa) was used to measure the pressure, and a receiving antenna (model LFL-1010 by Wellbrook Communications) connected to a spectrum analyzer was used to measure the frequency and power. The result plotted in Fig. 13 shows a stability of better than 0.05 dB over the range covering the regulation inflation pressures, and demonstrates that the inflation pressure of the football does not play a significant role in the transmit properties.

B. Force Test

During game-play, the football will be subjected to external pressure, such as when a player squeezes the ball or players lay on top of the ball. These actions could deform the ball and, thus, deform the loop antenna. To test the effect of this deformation, an apparatus was constructed, as shown in Fig. 12b, which allowed pressure to be applied across the center of the ball. A force measurement plate was used to determine the force on the ball. Wooden spacers were used to keep the ball separated from the metallic force plate, allowing a separation of approximately 45.4 cm. The power and frequency output from the integrated ball were measured using a using the same receiving setup as for the pressure test in the previous sub-section, and the results of these measurements are shown in Fig. 14. The results show power variations of up to 0.6 dB over a force range of 0 lbf to 170 lbf. Frequency variations were controlled to within 0.6 kHz. Based on experimental results from controlled measurements [1], we do not expect a variation of up to 0.6 dB to cause a large error in position or orientation, although the magnitude of the induced error must be studied in future work.

C. Dielectric Loading Test

Because the transmitter circuit and antenna were placed near the surface of the football, they will be in close proximity to lossy dielectric materials during use, i.e., the hand and arm of a football player. To simulate this effect, the integrated ball was held at a fixed position, and the power and frequency of the transmitter were measured while in close proximity to a human arm and hand. The following four tests were conducted: Two hands on the sides of the ball, one arm around the ball as shown in Fig. 12c, two arms holding the ball to the chest, and no dielectric contact to account for systematic

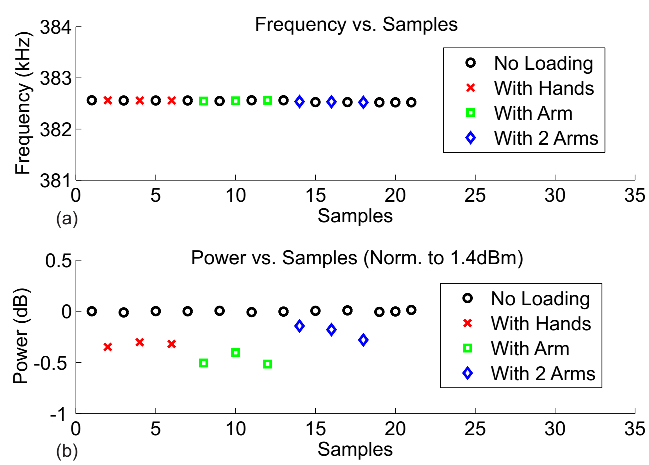

Fig. 15. The result of the dielectric loading test, showing the measured frequency (a) and power (b) as a function of different types of dielectric loading. The measurements were conducted by holding the ball using both hands, an arm, and both arms, and by comparing to the case where there were no dielectric loading.

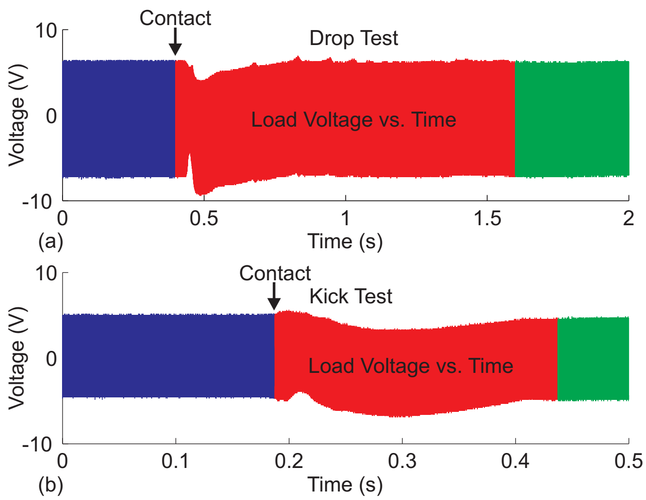

Fig. 16. The result of the impact test, showing the measured voltage when the football was dropped to the ground (a), and when the football was kicked (b), as a function of time. The region highlighted in red denotes where the football is observed to have contact with the ground and the kicker's foot.

changes in the transmitter's characteristics. The transmitter's power and frequency were measured using same setup used previously. Figure 15 shows the result for power and frequency variations of the transmitted magnetic field in the experiment. The measured frequency is shown to be almost constant, whereas the measured power varies by as much as 0.5 dB. We expect this to induce a small error in position and orientation determination, which must be further studied.

D. Impact Test

The football will be subjected to frequent impact in gameplay when, for example, the ball is kicked or when it hits the ground from a drop. To test the effect of impact on the transmitted fields, a ball was instrumented with the circuit external to the ball to allow access to the circuit for monitoring of the generated load voltage at the terminal of the antenna. The monitoring of the load voltage on the external circuit allowed us to see the changes in voltage caused by impact separate from those that would be caused by changes in the ball's position/orientation if the ball were monitored wirelessly. The voltage across the antenna was measured with an oscilloscope while the ball was dropped to the ground and while it was kicked. The ball was held in place with tape when the ball was kicked, as shown in Fig. 12d. The results in 16 show transient effects due to the impact caused by the kick and drop. The effects are not noticeable beyond the time where contact is visible (measured using a high-speed camera with 1000 fps). The load voltage is shown to largely return to its original value. More detailed testing is needed to study hysteresis effects associated with impact tests.

VI. Human Exposure Study

To determine whether or not the instrumented football was safe for testing with people, a preliminary study was conducted by the IT'IS Foundation to evaluate the instrumented ball's specific absorption rate (SAR) induced in a typical adult male [8]. The study did not consider the football's impact on implanted medical devices, and was done through simulation

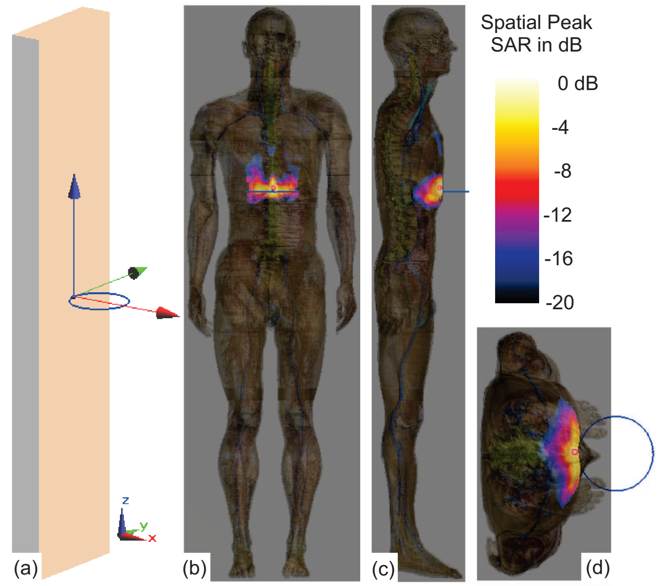

Fig. 17. The orientation of the simulated loop antenna with respect to the homogeneous phantom is shown in (a). The human model and the emitting loop antenna spaced 1 mm from the model's torso is shown in (b-d). This figure is modified from Fig. 1 and 6 in [8].

using the low-frequency (LF) solver in SEMCAD X v14.6 – a magnetoquasistatic solver implemented with the finite element method (FEM). The instrumented football was modeled as a single-turn, 163 mm-diameter loop with 8.5 Arms current. The current of 8.5 Arms was obtained from calculations based on a 50-turn 34 AWG loop carrying 170 mArms, which approximates the football transmitter. The value of 170 mArms is higher than that found in Section IIIb (159 mArms), and therefore represents a conservative estimate. Two simulations were conducted. In the first, the SAR exposure was calculated with the outer edge of the loop spaced a small distance from a homogeneous phantom – i.e., a rectangular volume whose homogeneous electromagnetic properties matched that of human muscle tissue – as shown in Fig. 17a. The separation distance was set to 0.5 mm, 1 mm, and 2 mm and the 1g peak spatial SAR (psSAR)[1] calculated. Then, to evaluate a worst case scenario, the 1g psSAR results were scaled to reflect a rectangular volume filled with cerebrospinal fluid (CSF) whose conductivity is much higher than muscle tissue. The results from this simulation are given in Table I. In the second simulation, the current-carrying loop was simulated in close proximity to a model of an adult, human male derived from magnetic resonance imaging (MRI) scans. The loop was spaced a distance of 1 mm from the torso of the human model, as shown in Fig. 17b-d, and the 1g psSAR and whole-body SAR results are shown in Table II. It can be seen that, for both simulations, the SAR result are at least one order of magnitude below the Federal Communications Commission (FCC) limits[2]. Therefore, this preliminary study suggests that the instrumented ball is safe for testing with people, excluding persons with implanted medical devices.

[1]The FCC SAR limits for general population/uncontrolled exposure are based on ANSI/IEEE standard C95.1-2005 [9] and state that the maximum SAR exposure is 0.08 W/kg averaged over the whole-body with the caveat that the psSAR cannot exceed 1.6 W/kg averaged over any 1 gram of tissue. For the hands, wrists, feet and ankles, the psSAR is limited to 4 W/kg averaged over any 10 grams of tissue.

TABLE I. EXPOSURE RESULTS FOR THE HOMOGENEOUS PHANTOM*

Distance (mm)	1g psSAR† (W/kg)		1g psSAR Relative to the FCC Limit (dB)	
	Muscle	CSF	Muscle	CSF
0.5	0.0177	0.0845	-19.6	-12.8
1.0	0.0162	0.0776	-19.9	-13.1
2.0	0.0139	0.0663	-20.6	-13.8

†Peak spatial SAR (psSAR) averaged over 1 gram of tissue
*This table is modified from Table 2 in [8].

TABLE II. EXPOSURE RESULTS FOR THE HUMAN MODEL‡

Frequency (kHz)	psSAR** (W/kg)		psSAR Relative to the FCC Limit (dB)	
	1g	Whole Body	1g	Whole Body
300	0.00314	7.08e-6	-27.1	-40.5
350	0.00432	9.85e-6	-25.7	-39.1
400	0.00572	1.31e-5	-24.5	-37.9

**Peak spatial SAR (psSAR)
‡This table is modified from Table 5 in [8].

VII. FOOTBALL TEAM DATA COLLECTION

The integrated football described in the previous sections was tested during a Carnegie Mellon University (CMU) varsity football team practice. During the practice, RF position estimates and video data were recorded for a combination of eighteen run and pass plays along with five choreographed plays. Reference points on the football field were recorded to define a mathematical transform relating physical locations on the football field to pixels in the fixed camera's view. The transform allowed the ball's position, as estimated by the RF system, to be overlaid on the camera view for the purpose of visualization. This section summarizes the setup used for the data collection and shows a visualization of one play.

A. Data Collection Setup

The experimental setup used to collect the RF data was identical to that described in previously published measurements [3] and further information about the hardware setup can be found in [2], [5]. To briefly summarize, the positions of the eight receiving antennas (which were measured with an optical surveying instrument) are shown in Fig. 1. The signal from each antenna was filtered, amplified, sampled with a bank of analog-to-digital converters, and stored for post-processing. The signal from each receiving antenna was sampled simultaneously at a rate of 10 MS/s during 5 ms windows. The sampled data was converted into the frequency domain and the power of the strongest frequency component was recorded for use in processing. The 5 ms sample windows were repeated so that the football's signal power was recorded simultaneously at each receiver at a rate of approximately 35 Hz. Therefore, a position estimate was generated for each frame of the video data which was recorded at a rate of 29.97 frames per second (fps). Estimating the football's position and orientation was posed as a nonlinear, least-square optimization problem [1]. A trust-region reflective optimization algorithm [10] (included in Matlab's [11] lsqnonlin function) was used to choose the position and orientation of the ball that minimized the difference between the measured and theoretical power, which was calculated using the known receiver positions, ground conductivity, and football transmit power.

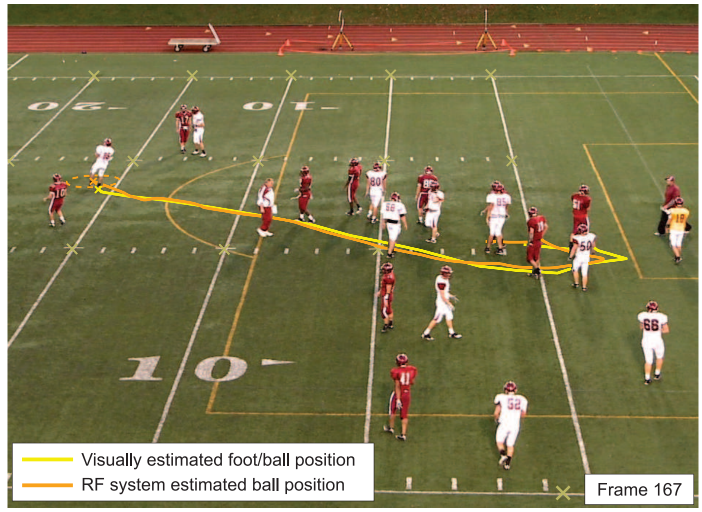

Fig. 18. The integrated football being used in running play in a CMU varsity football team practice. A visualization of the football's two-dimensional position trajectory, as estimated by the RF system, is compared to an estimate of the ball's true two-dimensional position trajectory.

In the plays recorded in the CMU football team practice, the position estimates were solved sequentially starting with the first collected set of power measurements and continuing to the last. For each football position and orientation estimate, the non-linear least-squares solver was run with 625 initial starting points to generate 625 intermediate results. The starting points formed a grid around the previous football position and orientation estimate and consisted of five values for x, y, ϕ (azimuth orientation), and θ (inclination angle, measured from the axis orthogonal to the plane of the football field). The height z of the starting point was equal to the previously estimated position of the ball. The final position estimate was chosen to be the intermediate result with the lowest cost function residual from the non-linear least-squares solver. Generating multiple intermediate results helped the solver avoid local minimas. When solving for the 625 intermediate results, the non-linear least-squares solver was allowed to search over a wide portion of the field. For the play shown in Fig. 18, the search space extended from the back of the end-zone to the 25 yard line and more than 7 yards past each sideline. The height of the search space was limited to 2.5 yards above the playing field and the orientation values were confined to $-\pi < \phi \leq \pi$ and $0 < \theta \leq 90$. The first initial starting point was selected by visually estimating the ball's position from the video data.

B. Data Collection Results

Fig. 18 shows the last frame (frame 167) from a video comparing the football's two-dimensional position trajectory, as estimated by the RF system, to an estimate of the ball's true two-dimensional position trajectory. Both trajectory estimates are shown projected into the plane of the football field. The orange ellipse is a 2-yard diameter circle projected into the plane of the football field to help qualitatively judge the accuracy of the RF position estimate. The full, three-dimensional position and orientation of the ball at each point along the trajectory was estimated; however, only the x and y position of the ball is shown here. The trajectory was estimated from

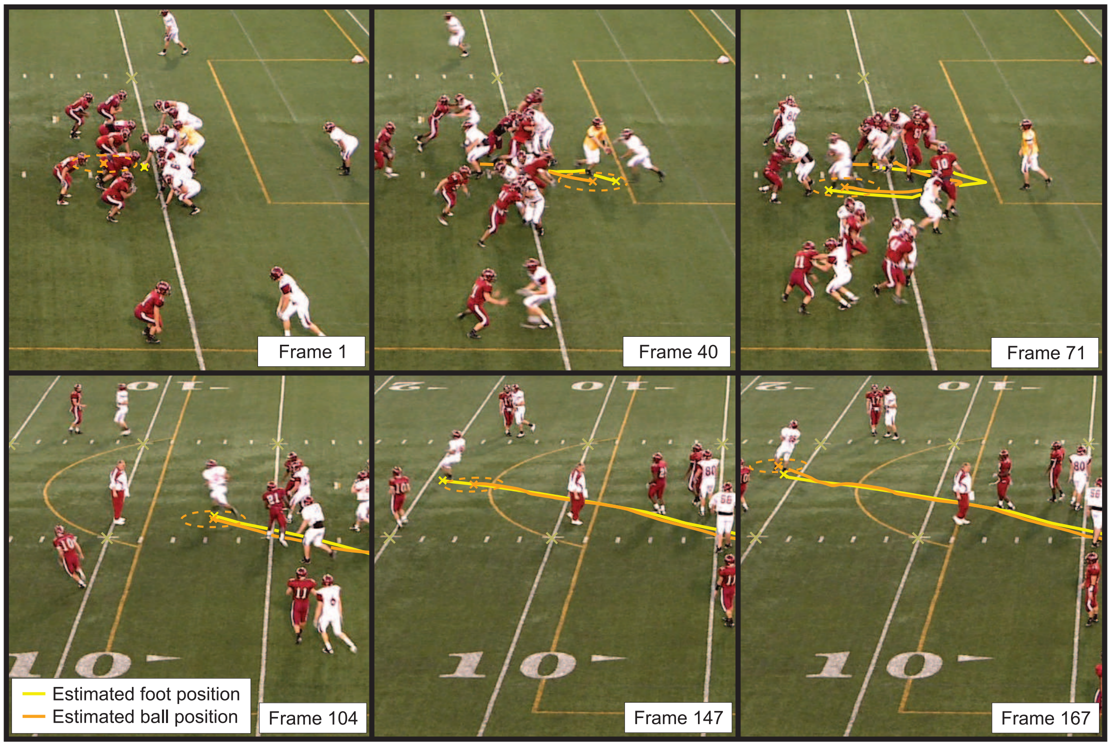

Fig. 19. Frames from a video of the run play shown in Fig. 18 comparing a visualization of the football's two-dimensional position trajectory, as estimated by the RF system, to an estimate of the ball's true two-dimensional position trajectory. Frames 1, 40, 71, 104, 147, and 167 (the final frame) are shown. The orange ellipse is a 2-yard diameter circle projected into the plane of the football field to help qualitatively judge the accuracy of the RF position estimate.

the RF data assuming that the electrical conductivity of the earth was 0.1 S/m. The ball's trajectory, as estimated by the RF system, was smoothed by applying Matlab's [11] robust, windowed least squares smoothing function with a window of 16 frames. The first few frames were not smoothed so that the ball's position did not drift in the video before the play started. The position of the player's feet were used as an estimate of the ball's true position trajectory in the plane of the football field. The foot of the player holding the ball that was closest to the ball and touching the grass was recorded. For video frames in which the position of the player's foot could not be seen or was not touching the ground, the estimated foot positions were interpolated from surrounding frames. In frames where the ball touched the ground, its position was marked instead of the player's foot.

The ball's trajectory as estimated by the RF system and the estimate of the true trajectory show good agreement in Fig. 18 and is further highlighted in Fig. 19, which shows selected frames from the video of the play. The position trajectories match qualitatively, although the snapshots in Fig. 19 indicate that the RF position estimate may lag the estimate of the ball's true position at times. This data collection demonstrates that the integrated ball can be used in game-play situations and provide estimates of the ball position, even when the the line-of-sight is blocked by multiple players.

VIII. Conclusion

A light-weight magnetoquasistatic tag is introduced that enables long-range, and accurate, position and orientation sensing, even when the LoS is blocked by large groups of people. We demonstrate its integration into an American football, and study its use during a collegiate American football game.

References

[1] D. Arumugam, J. Griffin, and D. Stancil, "Experimental Demonstration of Complex Image Theory and Application to Position Measurement," *IEEE Antennas Wireless Propag. Lett.*, vol. 10, pp. 282–285, April 2011.

[2] D. Arumugam, J. Griffin, D. Stancil, and D. Ricketts, "Three-Dimensional Position and Orientation Measurements using Magneto-quasistatic Fields and Complex Image Theory," *IEEE Trans. Antennas and Propogation*, submitted.

[3] ——, "Magnetoquasistatic Tracking of an American Football: A Goal Line Measurement," *IEEE Antennas and Propagation Magazine*, submitted.

[4] C. Santiago, A. Sousa, M. Estriga, L. Reis, and M. Lames, "Survey on Team Tracking Techniques Applied to Sports," in *2010 International Conference on Autonomous and Intelligent Systems (AIS)*, June 2010, pp. 1 – 6.

[5] D. Arumugam, J. Griffin, D. Stancil, and D. Ricketts, "Two-dimensional position measurement using magnetoquasistatic fields," *Antennas and Propagation in Wireless Communications (APWC), 2011 IEEE-APS Topical Conference on*, pp. 1193–1196, Sept. 2011.

[6] "Official Playing Rules and Casebook of the National Football League," 2012. [Online]. Available: http://www.nfl.com/rulebook

[7] M. Kazimierczuk, V. Krizhanovski, J. Rassokhina, and C. D.V., "Class-E MOSFET Tuned Power Oscillator Design Procedure," *IEEE Trans. on Circuits and Systems*, vol. 52, no. 6, pp. 1138–1147, 2005.

[8] J. Nadakuduti, M. Douglas, and N. Kuster, "Evaluation of Position Location System with Respect to EM Exposure Limits," ITIS Foundation – Foundation for Research on Information Technologies in Society, Zürich, Switzerland, Tech. Rep. 0363B, January 2012.

[9] "IEEE Standard for Safety Levels With Respect to Human Exposure to Radio Frequency Electromagnetic Fields, 3 kHz to 300 GHz," *IEEE Std C95.1-2005 (Revision of IEEE Std C95.1-1991)*, pp. 1 – 238, 2006.

[10] T. Coleman and Y. Li, "An interior trust region approach for nonlinear minimization subject to bounds," *SIAM Journal on Optimization*, vol. 6, no. 2, pp. 418–445, 1996.

[11] "Mathworks, Inc." 2012, accessed January, 2013. [Online]. Available: http://www.mathworks.com